HAL
open science

Heteroepitaxy of Scandium Delafossite on ZnO

Stéphane Grenier, Fabrice Donatini, Eric Mossang, Pierre R. Muret

To cite this version:

Stéphane Grenier, Fabrice Donatini, Eric Mossang, Pierre R. Muret. Heteroepitaxy of Scandium Delafossite on ZnO. physica status solidi (b), 2022, 259 (8), pp.2200044. 10.1002/pssb.202200044 . hal-03450008

HAL Id: hal-03450008

https://hal.science/hal-03450008v1

Submitted on 25 Nov 2021

HAL is a multi-disciplinary open access archive for the deposit and dissemination of scientific research documents, whether they are published or not. The documents may come from teaching and research institutions in France or abroad, or from public or private research centers.

L'archive ouverte pluridisciplinaire **HAL**, est destinée au dépôt et à la diffusion de documents scientifiques de niveau recherche, publiés ou non, émanant des établissements d'enseignement et de recherche français ou étrangers, des laboratoires publics ou privés.

Heteroepitaxy of Scandium delafossite on ZnO

S. Grenier, F. Donatini, E. Mossang, and P. Muret

Institut Néel, Centre National de la Recherche Scientifique

& Université Grenoble Alpes

Grenoble, France

(Dated: 24 February 2021)

Abstract

The trigonal polytypes of the delafossites $ScCuO_{2+\delta}$ and $Sc_{1-x}Mg_xCuO_{2+\delta}$, which are p-type semiconductors, are elaborated by pulse laser deposition and epitaxially grown on the oxygen terminated $(00\bar{1})$ ZnO surface along their same basal plane with an absolute mismatch less than 0.5 %. Depending on the Mg content x and excess intercalated oxygen δ, the relative mismatch can be either positive or negative, but very close to zero in any cases. Optically excited transitions between valence band and conduction band states detected from spectroscopic ellipsometry and cathodoluminescence spectrum confirm the band structure calculated theoretically by several authors. The deviation between fundamental optical absorption and exciton radiative recombination yields an exciton binding energy of 0.2 eV.

Keywords: heteroepitaxy; delafossite; optical properties

I. INTRODUCTION

ZnO is a semiconductor with potentially attractive optical properties for numerous optoelectronic applications, especially if optimal doping can be achieved[1]. While n-type doping can be obtained with high donor concentrations, p-type doping instead has never reached a robust and sufficient level, neither in bulk crystals nor in monocrystalline films. Such difficulties are linked to the fundamental physics of defects, with a lower formation energy for those which compensate acceptors, also known as "hole killer", thus preventing the Fermi level from approaching the valence band maximum, as supported by a phenomenological model[2] and by theoretical calculations[3]. For example, high quality epitaxial films doped with nitrogen, one element among the best candidates for p-type doping, either stay n-type with a large number of deep defects on both sides of the bandgap[4], or show a weak transient p-type doping that finally return to n-type[5]. Whereas p-type doping has been evidenced, near surfaces, at grain boundaries in polycrystalline material[6] and in nanopillars[7], doping homogeneity and high concentrations of holes, necessary to electroluminescent diodes and most optoelectronic applications, remain out of reach. On the contrary, most copper delafossites $CuXO_2$ (X being a trivalent element), which are semi-conducting oxides with hexagonal or trigonal structure, are naturally p-type[8,9]. Although a general rule is still not clear, several properties which contribute to enhance the hole concentration have been discovered. These are the combination of a trivalent ion of a sufficient size, interstitial intercalation of oxygen into Cu planes[10,11], substitution of divalent ions for a small percentage of trivalent ones[10–14], and copper vacancies[15]. From these studies, $CuXO_2$ appeared more and more conductive with X=Y, Sc, Cr in this order. Among these three oxides, [2H]$CuScO_2$ and [3R]$CuScO_2$ have a basal plane (0001) which fits the same basal plane of ZnO with a very low mismatch of less than 1 %, but epitaxial films have been deposited only on sapphire[11,16] or spinel[17], with an epitaxial relationship less straightforward and a larger mismatch. To achieve better interface quality, an atomic structure with a minimum distortion across the interface is highly recommended, thus minimizing interface defects and optimizing the electrical properties of the heterojunction. This is the aim of the present study, which demonstrates the heteroepitaxy of [3R]$CuScO_{2+\delta}$ and [3R]$CuSc_{1-x}Mg_xO_{2+\delta}$ on ZnO.

II. EXPERIMENTAL

Either commercial ZnO crystals grown by the hydrothermal method or wafers grown by the chemical vapour transport method from a partner team[18] are used as substrates. Deposition is done on the oxygen terminated $(00\bar{1})$ face, after recrystallization of the polished surface performed by annealing at 1200 ℃ one hour under pure oxygen at atmospheric pressure. The direction normal to the surface plane of ZnO crystals is thus colinear with the c axis. A target with stoichiometric composition, 20 mm in diameter, is elaborated by mixing hydrated copper and scandium nitrates containing known numbers of water molecules, followed by sintering and heating twice the mixture at 1200 ℃ in air. Powder diffraction diagram shows peaks of [2H]$CuScO_2$, [3R]$CuScO_2$, [2H]$CuScO_{2.5}$ and [3R]$CuScO_{2.5}$. Pulsed laser deposition is performed in a vessel equipped with an electron cyclotron resonance (ECR) source of atomic oxygen operating with a power of 60 W at 2.45 GHz under a magnetic field of 845 gauss, and delivering mainly excited neutral oxygen atoms with a pressure of 3 mtorr in the chamber. The ECR source can be idle to serve as a feedthrough when a higher pressure of molecular oxygen is required. However, pressures above 10 mtorr are found detrimental to the deposition rate. The laser beam is focused on the target through an external lens after reflection on three mirrors, illuminating a rectangle approximately 3 mm high and 1.5 mm wide at a wavelength of 248 nm, with 25 ns duration for each pulse. With typical energy of 230 mJ per pulse, the density on the target is close to 5 $J.cm^{-2}$. The repetition rate is one shot per second. A set-up behind the last mirror slightly moves it to change the impact location of the beam on the target. Inside the vessel, four targets are mounted on a carousel, one with $CuScO_2$, one with MgO, an other with CuO, thus allowing incorporation of magnesium rather than scandium into the film. The elaboration of the film is performed sequentially, alternating deposition of material necessary to build two unit cells of $CuSc_{1-x}Mg_xO_2$ at 875 ℃ and annealing under an enhanced oxygen pressure, generally 100 mtorr. These two steps are repeated up to a thickness of about 100 nm. However, post-annealing the sample one hour under an oxygen pressure of 10 torr at 900 ℃ is necessary to strongly improve the crystalline structure of the film. Cooling is achieved with a typical rate of 40 ℃ per mn with a pause at 500 ℃ during two hours to incorporate interstitial oxygen atoms in the Cu planes[19].

X-ray diffraction was performed either on a Bruker D8 Discover diffractometer using both

the CuKα1 and CuKα2 radiations at a wavelength of 1.5418 Å, or a high resolution Smart-Lab X-ray diffractometer (Rigaku) consisting of a 9 kW rotating Cu anode and a 5-circle goniometer. With the later, the incident X-ray beam was monochromatised with a 2-bounce Ge(220) crystal (wavelength of 1.5405 Å for the CuKα1 radiation). Spectroscopic ellipsometry is achieved in an alpha-SE ellipsometer from the Woolam company, equipped with the EASE software for data analysis. Cathodoluminescence measurements are performed in a scanning electron microscope FEI Inspect F50 equipped with a parabolic collecting mirror with a hole located at the electron beam axis. The spectroscopy of the light emitted by the sample is performed using a UV-enhanced optical system.

III. STRUCTURAL CHARACTERIZATION

In all the films of $CuSc_{1-x}Mg_xO_{2+\delta}$ elaborated on the $(00\bar{1})$ surface of ZnO substrates, only $(00l)$ peaks are detected in the $\theta - 2\theta$ diagrams obtained in specular configuration, indicating that $(00l)$ planes of the delafossite are parallel to those of ZnO (Figure 1), whatever the polytype really elaborated, when the representation using hexagonal lattice parameters of the trigonal lattice is adopted.

To know what polytype has epitaxially grown, a phi-scan is performed at $2\theta = 53.8°$, showing the specific (018) peak of the trigonal delafossite, whereas no peak exists at this 2θ angle in the hexagonal polytype. By contrast, the (018) peak of the hexagonal polytype would be found near $2\theta = 74$ °, very far from that evidenced in Figure 2.

Sixfold multiplicity of the planes belonging to the $\{110\}$, $\{\bar{1}20\}$ and $\{\bar{2}10\}$ families[20], perpendicular to the c-axis, is checked with the help of diffraction at glancing incidence with the detector at $2\theta_\chi = 57.4°$, since the periodicity of the peaks appearing in the phi-scan diagram amounts to 360°/6 =60° (Figure 3). From the plane (110), such a rotation around the c-axis allows to shift sequentially to $(\bar{1}20)$, $(\bar{2}10)$, $(\bar{1}\bar{1}0)$, $(1\bar{2}0)$ and $(2\bar{1}0)$ in this order, like in the ZnO substrate. Oxygen atoms belong to these planes and form hexagonal sets like in hexagonal ZnO, also on its surface since the substrate is oxygen terminated. But the entire lattice of the delafossite is invariant through rotations of 120° in accordance with the space group R - 3 m. Because these oxygen hexagonal sets located at the interface are common to the two crystals, the epitaxial relationships should be either $CuSc_{1-x}Mg_xO_{2+\delta}$[100]//ZnO[100] or $CuSc_{1-x}Mg_xO_{2+\delta}$ [100]//ZnO[110].

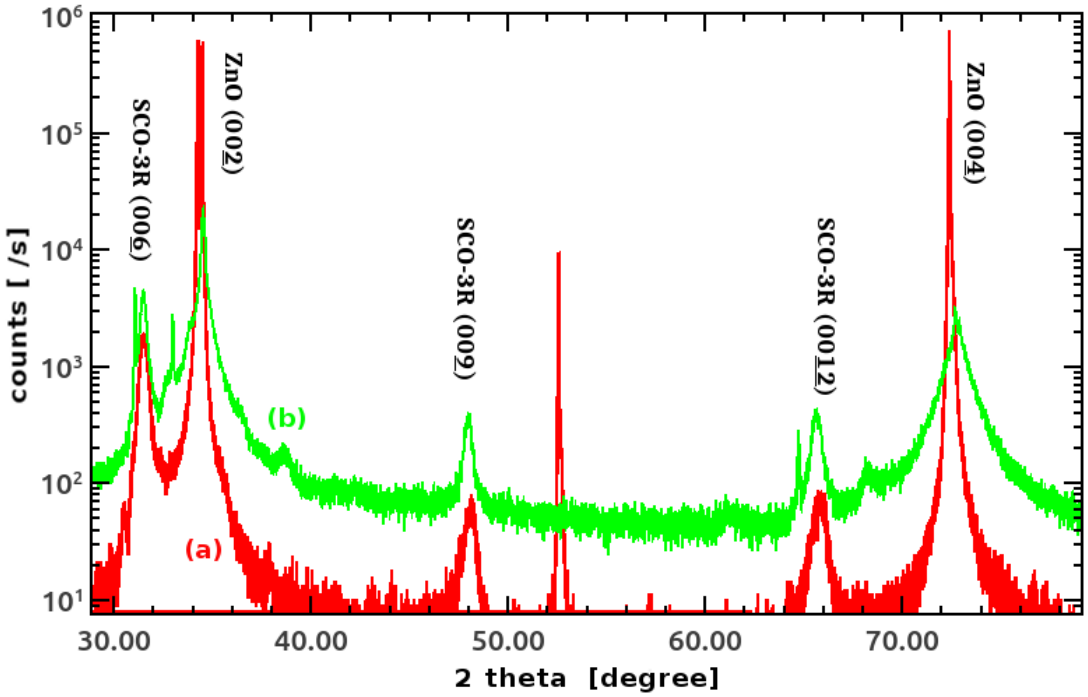

FIG. 1. $\theta - 2\theta$ X-ray diffraction diagrams for (a) $CuSc_{0.975}Mg_{0.025}O_{2+\delta}$ with high resolution and background near 10 counts/s and (b) $CuScO_{2+\delta}$ at low resolution and background near 10^2 counts/s. Delafossite peaks are labeled SCO-3R (00l).

In both delafossite polytypes, the two parameters which define the size of the unit cell are c along the c axis and a for the two axes inside the basal plane, making an angle of 120° between them. To know whether the delafossite lattice is either pseudomorphic or relaxed, diffraction on planes $\{0kl\}$, $\{hkl\}$ or $\{hk0\}$ is needed in order to measure the a parameter. Diffraction on planes (110) is performed at glancing incidence with two angles, 0.5° and 0° in $\theta - 2\theta$ configuration (Figure 4). In the first case, both crystals contribute while in the second case, the beam enters the trench of the ZnO crystal and only the ZnO planes participate to the diffracted beam. By difference, the peak due to the delafossite (110) planes is well identified and its position allows the accurate determination of the a parameter. Diffraction by other $\{0kl\}$ planes are also used. In comparison to the stoichiometric compound [3R]$CuScO_2$, substitution of divalent cations like Mg contribute to decrease the a parameter because of a smaller ionic radius while intercalation of oxygen into Cu planes has an opposite effect[19,21]. Measured parameters for the ZnO substrate, three delafossite thin

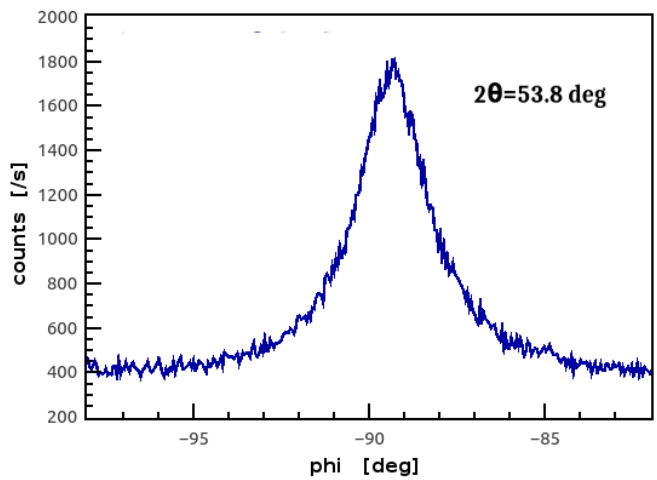

FIG. 2. Phi-scan at glancing incidence and $\theta - 2\theta$ configuration with $2\theta = 53.8°$, selecting the (018) planes.

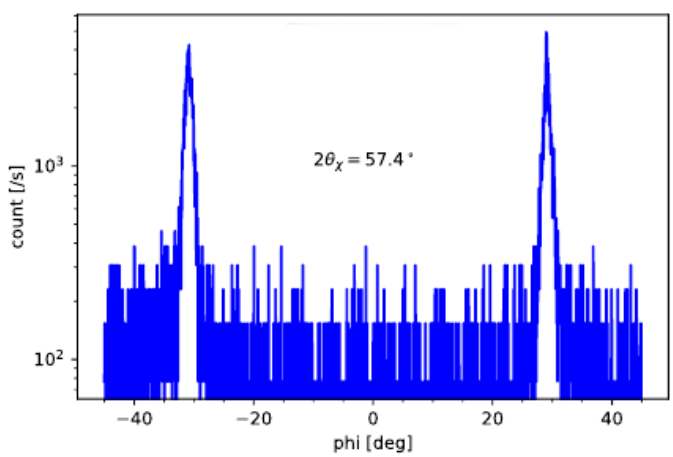

FIG. 3. Phi-scan at glancing incidence and $2\theta_\chi = 57.4°$, selecting the $\{110\}$, $\{\bar{1}20\}$ and $\{\bar{2}10\}$ plane families.

films with different substitutions of Mg for Sc and those given in literature are displayed in Table I. In the column da/a, the relative misfit between the a parameters of the substrate and the film is indicated. The decrease of the c parameter due to a weak bond between oxygen atoms intercalated in Cu planes and Sc atoms in comparison to the stoichiometric compounds is confirmed.

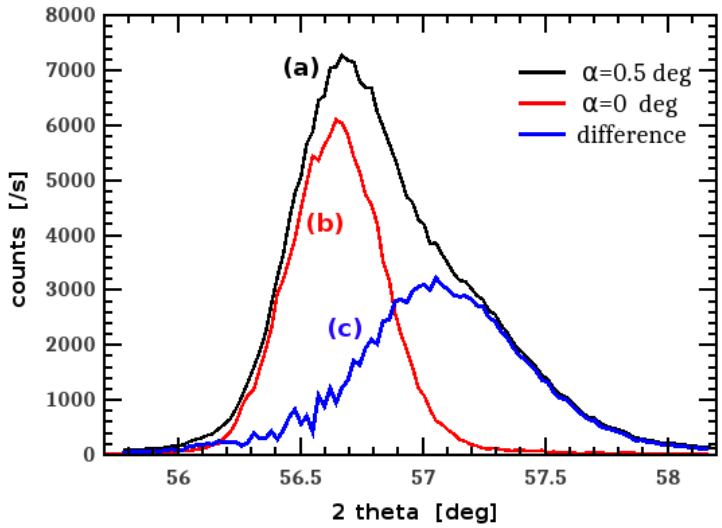

FIG. 4. $\theta - 2\theta$ scan near $2\theta = 57°$ at two glancing incidences: (a) $\alpha = 0.5°$ and (b) $\alpha = 0°$. Since only the ZnO substrate contributes in case (b), the difference (c) yields the specific peak of the (110) planes in the delafossite.

Table I

materials	c (Å)	a (Å)	da/a	δ
ZnO †	5.198±0.004	3.248±0.004	—	—
$CuScO_{2+\delta}$ †	17.058±0.012	3.26±0.01	+0.37%	0.36
$CuSc_{0.985}Mg_{0.015}O_{2+\delta}$ †	17.015±0.02	3.24±0.02	−0.24%	0.47
$CuSc_{0.975}Mg_{0.025}O_{2+\delta}$ †	17.021±0.010	3.23±0.02	−0.46%	0.23
bulk $CuScO_2$[19–21] ‡	17.097	3.219	—	0
bulk $CuScO_{2.5}$[19,21] ‡	17.039	3.269	—	0.5

†this study

‡average of the data given in the references

It seems that all the films are relaxed despite absolute deviation of each a parameter always less than 0.5% from that of ZnO. However, such a conclusion assumes a perfect homogeneity of the a parameter from the interface up to the film surface, a fact which is not checked and leaves occasionally the possibility of a pseudomorphic heteroepitaxy in the first film layers if strain exists in them and above. Assuming linear relationships between parameters, Mg content x like in $CuCr_{1-x}Mg_xO_2$[22] and oxygen content[19,21] δ, the intercalated

excess oxygen can be estimated and is indicated in the last column of Table I. It appears that the two quantities x and δ are able to control the a parameter. Therefore, if a further decrease of the heteroepitaxy misfit is suitable, an even more meticulous structural study would be needed. But a perfect pseudomorphism can certainly be obtained since the present study demonstrates that the a parameter of the $CuSc_{1-x}Mg_xO_{2+\delta}$ films can be either larger or smaller than that of ZnO.

IV. OPTICAL PROPERTIES

The optical responses of the films and of the multilayer comprising the film and the ZnO substrate are investigated both by spectroscopic ellipsometry and cathodoluminescence. In the first case, changes in the ellipticity and angle of a light beam, linearly polarized and directed to the samples surface with an incidence angle of 45°, are collected from $h\nu =$ 0.7 eV to 5.8 eV. The same is done on bare substrates, allowing the extraction of the film response alone. Then, the film data are fitted with the help of four oscillators inside the measured energy range and a Drude contribution due to hole conduction, plus two oscillators outside the measured energy range, one in the mid-infrared and the other above 5.8 eV. The optical parameters of the delafossite films are obtained from the best fit. If the Drude contribution is canceled, a shift of the whole simulated response appears in comparison to the experimental one, indicating that the film conductivity exceeds 10 $\Omega^{-1}cm^{-1}$, with hole concentrations probably above 10^{20} cm^{-3} because of the low mobility. Such a property matches the experimental findings in bulk polycrystalline materials[10,12].

Optical absorption is of paramount importance because it can be compared to the band structure of the material and can thus confirm its identification. Here, the imaginary part ε_2 of the dielectric permittivity is deduced from the analysis of spectroscopic ellipsometry and plotted as a function of photon energy (Figure 5). Some authors[24,25] have determined either this quantity or absorption coefficient among those who have done *ab initio* calculations of the band structure for several copper delafossite compounds[26–28]. A less accurate but simpler model, which relies on the joined density of states (JDOS) calculated from the Scanlon study[23], is used here. The forbidden band gap energy is the single parameter which has been adjusted to 3 eV in order that peak extrema fit experimental optical absorption

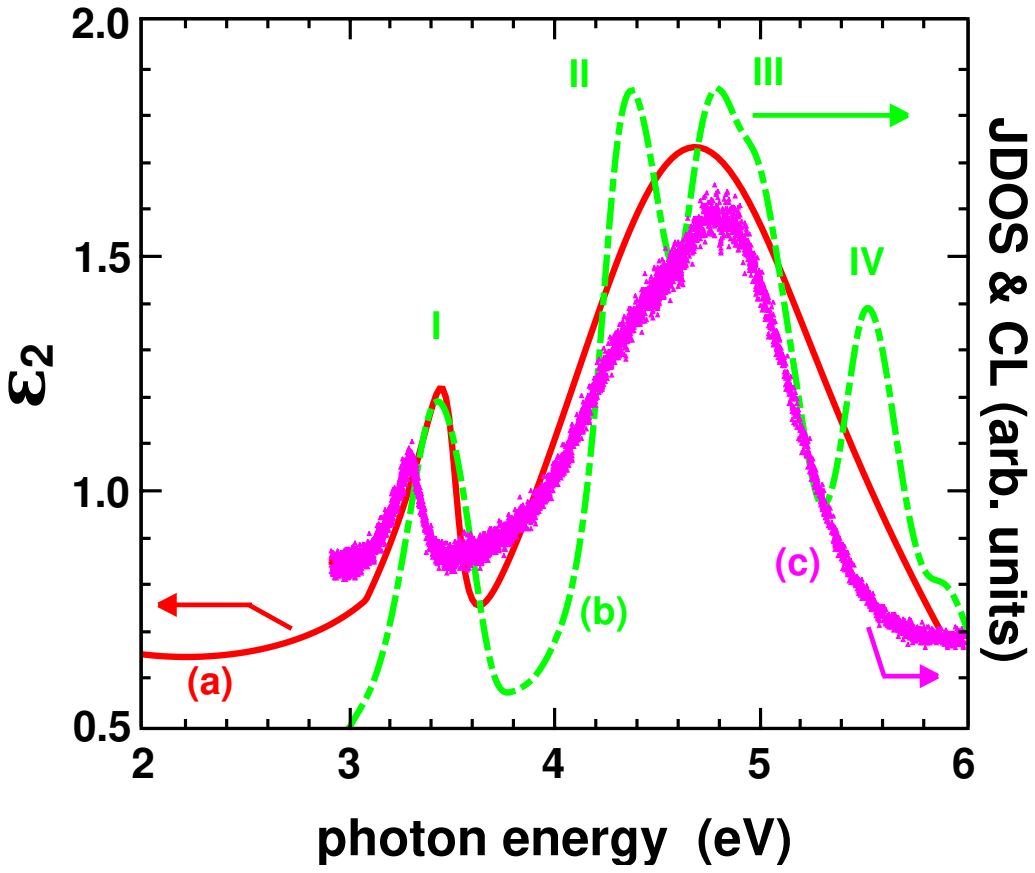

FIG. 5. (a) Imaginary part ε_2 of the film permittivity ; (b) Joined density of states (JDOS) calculated from Scalon *et al.*[23]; (c) cathodoluminescence intensity (CL) of light emitted by the film at room temperature under 4 keV electron bombardment.

featured by ε_2 the best way. Excepted when electronic transitions from states belonging to the valence band into empty states of the conduction band are forbidden by selection rules, JDOS approximates their strength with a good accuracy for the extrema position on the energy scale. This is the case for the three peaks numbered I, II and III in Figure 5, mainly due to transitions from oxygen 2p to Sc 3d states, in accordance with the structure of the optical absorption calculated by Shi[25], whereas the fourth does not induce optical absorption probably because the transition is forbidden between 3d states of Cu and empty 3d states of Sc. In experimental ε_2, a single wide peak appears at 4.65 eV rather than the two JDOS peaks II and III, respectively at 4.4 and 4.8 eV, because the effective ellipsometric response mixes $\varepsilon_{2\perp}$ and $\varepsilon_{2//}$ due to the 45° incidence angle of the beam with the surface. As the peaks II and III are slightly shifted in calculated $\varepsilon_{2\perp}$ and $\varepsilon_{2//}$[24], a single maximum results.

On the contrary, in the cathodoluminescence experiment, the light beam is collected close to the normal to the surface, favoring $\varepsilon_{2\perp}$ almost exclusively and producing a spectrum with a better resolution for the II and III structures, the former appearing as a shoulder near 4.4 eV as predicted by JDOS (see Figure 5). In this experiment, the electron beam is accelerated under 4 keV to localize the interactions only inside the film, before the buried interface with the substrate. The structure I is well marked close to 3.4 eV both in JDOS and ε_2 while the cathodoluminescence structure is red shifted near 3.2 eV. This deviation comes from the fundamental difference between the two physical mechanisms at stake respectively in ellipsometry and cathodoluminescence measurements. In the second case, the interaction of the electron beam with the film takes place inside a volume extending over dimensions less than 100 nm and creates many secondary electrons for each incident electron. Then, excitons can easily form and there radiative recombination produces luminescence, whereas in ellipsometry measurements, electron concentration due to optical absorption in the first nanometers beneath the film surface over an area of several mm^2 cannot reach a sufficient level to trigger exciton formation. Therefore, the exciton binding energy in $CuSc_{1-x}Mg_xO_{2+\delta}$ turns out to be the difference between the two peaks, namely close to 0.2 eV, while predicted values in transition metal delafossites[29] appear to be in the range 0.24 to 0.44 eV. It is not clear why both the exciton peak energy and binding energy are markedly higher in reference [17] than our experimental values but the optical response shown by these authors is also far from the JDOS, contrary to what is evidenced in our study. Moreover, the plot of $(\alpha h\nu)^2$ (not shown), where α is the absorption coefficient, yields an intercept with the photon energy axis near 3 eV, which is both the expected value for the forbidden bandgap like in reference [25] and that adjusted in JDOS to fit our experimental ε_2. All these optical properties confirm the nature of the films.

V. CONCLUSIONS

In this study, we have reported the heteroepitaxy of $ScCuO_{2+\delta}$ and $Sc_{1-x}Mg_xCuO_{2+\delta}$ films, about 100 nm thick, elaborated by pulse laser deposition onto the basal plane $(00\bar{1})$ of ZnO, where the same hexagonal sets of oxygen atoms exist as in the delafossites of either polytypes. It is demonstrated that only the trigonal polytype has grown in our samples. Post annealing of the samples allows to increase the interstitial oxygen content

which is intercalated into the Cu planes, thus increasing the a parameter, rising the positive charge on the Cu ions toward +2 and increasing the hole concentration, as checked from the ellipsometry analysis. The substitution of Mg for Sc may also participate to the increase of hole concentration and allows to decrease the parameters of the unit cell. A fine tuning of the heteroepitaxy matching becomes possible in this way. Optical properties measured by spectroscopic ellipsometry and cathodoluminescence confirm the band structure calculations published in the literature and comparison of the fundamental absorption and excitonic recombination energies yields an exciton binding energy of 0.2 eV, slightly below the high values predicted in literature by *ab initio* calculations. Such heterostructures can open a route to pn heterojunctions on n-type ZnO. Other compositions based on alloys of yttrium and 3d[30] or 4d transition metals delafossite, preserving the same R - 3 m space group of the mixed compound and a parameter a still close to that of ZnO, could be useful for elaborating multilayers able to show electroluminescence in the visible range.

ACKNOWLEDGMENTS

We wish to acknowledge the support of Jérôme Debray for his high skill work intended to polish and reclaim ZnO substrates and David Eon for his introduction to spectroscopic ellipsometry measurements. We are very grateful to David Barral and Arnaud Claudel for their technical assistance, to Laurent Ranno and Thibaut Devillers for their advices, deposition facilities improvement and training in laser control, and to Nora Dempsey who has permitted utilization of the pulsed laser deposition equipment. The LANEF framework (No. ANR-10-LABX-51-01) is acknowledged for its support with the mutualized Smartlab.

REFERENCES

[1]. Özgür, Y. I. Alivov, C. Liu, A. Teke, M. A. Reshchikov, S. Dogan, V. Avrutin, S.-J. Cho, and H. Morkoç, "A comprehensive review of ZnO materials and devices," Journal of Applied Physics **98**, 041301 (2005).

[2]S. Zhang, S.-H. Wei, and A. Zunger, "A phenomenological model for systematization and prediction of doping limits in II-VI and I-III-VI_2 compounds," Journal of Applied Physics **83**, 3192–3196 (1998).

[3]J. Robertson and S. J. Clark, "Limits to doping in oxides," Physical Review B **83**, 075205 (2011).

[4]P. Muret, D. Tainoff, C. Morhain, and J.-M. Chauveau, "Donor and acceptor levels in ZnO homoepitaxial thin films grown by molecular beam epitaxy and doped with plasma-activated nitrogen," Applied Physics Letters **101**, 122104 (2012).

[5]D. Wang, J. Zhang, Y. Peng, Z. Bi, X. Bian, X. Zhang, and X. Hou, "Plasma-activated nitrogen-doped p-type ZnO thin films with multi-buffer-layers grown on sapphire (0 0 0 1) by L − MBE," Journal of alloys and compounds **478**, 325–329 (2009).

[6]D. F. Urban, W. Körner, and C. Elsässer, "Mechanisms for p-type behavior of ZnO, $Zn_{1-x}Mg_xO$, and related oxide semiconductors," Physical Review B **94**, 075140 (2016).

[7]E. Latu-Romain, P. Gilet, N. Chevalier, D. Mariolle, F. Bertin, G. Feuillet, G. Perillat-Merceroz, P. Ferret, F. Levy, P. Muret, *et al.*, "Surface-induced p-type conductivity in ZnO nanopillars investigated by scanning probe microscopy," Journal of Applied Physics **107**, 124307 (2010).

[8]R. Nagarajan, N. Duan, M. Jayaraj, J. Li, K. Vanaja, A. Yokochi, A. Draeseke, J. Tate, and A. Sleight, "p-type conductivity in the delafossite structure," International Journal of Inorganic Materials **3**, 265–270 (2001).

[9]M. A. Marquardt, N. A. Ashmore, and D. P. Cann, "Crystal chemistry and electrical properties of the delafossite structure," Thin Solid Films **496**, 146–156 (2006).

[10]R. Nagarajan, A. Draeseke, A. Sleight, and J. Tate, "p-type conductivity in $CuCr_{1-x}Mg_xO_2$ films and powders," Journal of Applied Physics **89**, 8022–8025 (2001).

[11]Y. Kakehi, K. Satoh, Y. Tsutom, Y. Takeshi, A. Ashida, and N. Fujimura, "Epitaxial growth of $CuScO_2$ thin films on sapphire a -plane substrates by pulsed laser deposition," Journal of Applied Physics **97**, 083535 (2005).

[12]J. Tate, M. Jayaraj, A. Draeseke, T. Ulbrich, A. Sleight, K. Vanaja, R. Nagarajan, J. F. Wager, and R. Hoffman, "p-type oxides for use in transparent diodes," Thin solid films **411**, 119–124 (2002).

[13]Y. Kakehi, K. Satoh, T. Yoshimura, A. Ashida, and N. Fujimura, "Control of carrier concentration of p-type transparent conducting $CuScO_2$ (0001) epitaxial films," Thin Solid Films **518**, 3097–3100 (2010).

[14]T. Okuda, N. Jufuku, S. Hidaka, and N. Terada, "Magnetic, transport, and thermoelectric properties of the delafossite oxides $CuCr_{1-x}Mg_xO_2$ (x from 0 to 0.04)," Physical Review

B **72**, 144403 (2005).

[15]P. L. Popa, J. Crepelliere, P. Nukala, R. Leturcq, and D. Lenoble, "Invisible electronics: Metastable Cu−vacancies chain defects for highly conductive p-type transparent oxide," Applied Materials Today **9**, 184–191 (2017).

[16]Y.-H. Chuai, H.-Z. Shen, Y.-D. Li, B. Hu, Y. Zhang, C.-T. Zheng, and Y.-D. Wang, "Epitaxial growth of highly infrared-transparent and conductive $CuScO_2$ thin film by polymer-assisted-deposition method," RSC Adv. **5**, 49301–49307 (2015).

[17]H. Hiraga, T. Makino, T. Fukumura, A. Ohtomo, and M. Kawasaki, "Excitonic characteristics in direct wide-band-gap $CuScO_2$ epitaxial thin films," Applied Physics Letters **95**, 211908 (2009).

[18]J.-L. Santailler, C. Audoin, G. Chichignoud, R. Obrecht, B. Kaouache, P. Marotel, D. Pelenc, S. Brochen, J. Merlin, I. Bisotto, C. Granier, G. Feuillet, and F. Lévy, "Chemically assisted vapour transport for bulk ZnO crystal growth," Journal of Crystal Growth **312**, 3417 – 3424 (2010).

[19]J. Li, A. F. Yokochi, and A. W. Sleight, "Oxygen intercalation of two polymorphs of $CuScO_2$," Solid state sciences **6**, 831–839 (2004).

[20]J. P. Doumerc, A. Ammar, A. Winchainchai, M. Pouchard, and P. Hagenmuller, "Sur quelques nouveaux composes de structure de type delafossite," Journal of Physics and Chemistry of Solids **48**, 37 – 43 (1987).

[21]O. Garlea, P. Bordet, C. Darie, O. Isnard, and R. Ballou, "$InCuO_{2.5}$ and $ScCuO_{2.5}$: new oxidized copper delafossites with triangular lattices of Cu^{2+} cations," Journal of Physics: Condensed Matter **16**, S811 (2004).

[22]P. Sadik, M. Ivill, V. Craciun, and D. Norton, "Corrigendum to"electrical transport and structural study of $CuCr_{1-x}Mg_xO_2$ delafossite thin films grown by pulsed laser deposition"[thin solid films 517 (2009) 3211-3215]," TSF **518**, 3439–3439 (2010).

[23]D. O. Scanlon, K. G. Godinho, B. J. Morgan, and G. W. Watson, "Understanding conductivity anomalies in Cu–I-based delafossite transparent conducting oxides: Theoretical insights," The Journal of chemical physics **132**, 024707 (2010).

[24]R. Gillen and J. Robertson, "Band structure calculations of $CuAlO_2$, $CuGaO_2$, $CuInO_2$, and $CuCrO_2$ by screened exchange," Physical Review B **84**, 035125 (2011).

[25]L.-J. Shi, Z.-J. Fang, and J. Li, "First-principles study of p-type transparent conductive oxides $CuXO_2$ (X = Y, Sc, and Al)," Journal of Applied Physics **104**, 073527 (2008).

[26]F. Trani, J. Vidal, S. Botti, and M. A. Marques, "Band structures of delafossite transparent conductive oxides from a self-consistent GW approach," Physical Review B **82**, 085115 (2010).

[27]R. Laskowski, N. E. Christensen, P. Blaha, and B. Palanivel, "Strong excitonic effects in $CuAlO_2$ delafossite transparent conductive oxides," Physical Review B **79**, 165209 (2009).

[28]M. N. Huda, Y. Yan, A. Walsh, S.-H. Wei, and M. M. Al-Jassim, "Group-IIIA versus IIIB delafossites: Electronic structure study," Physical Review B **80**, 035205 (2009).

[29]X. Wang, W. Meng, and Y. Yan, "Electronic band structures and excitonic properties of delafossites: A $GW - BSE$ study," Journal of Applied Physics **122**, 085104 (2017).

[30]H. Hiraga, T. Makino, T. Fukumura, H. Weng, and M. Kawasaki, "Electronic structure of the delafossite-type $CuMO_2$ (M = Sc, Cr, Mn, Fe, and Co): Optical absorption measurements and first-principles calculations," Physical Review B **84**, 041411 (2011).